Linear Model Predictive Control for Schrödinger Equation

Citation
Humaloja, J-P., & Dubljevic, S. (2018). Linear Model Predictive Control for Schrödinger Equation. In *2018 Annual American Control Conference, ACC 2018* (pp. 2569-2574). IEEE.
https://doi.org/10.23919/ACC.2018.8431686

Year
2018

Version
Peer reviewed version (post-print)

Link to publication
TUTCRIS Portal (http://www.tut.fi/tutcris)

Published in
2018 Annual American Control Conference, ACC 2018

DOI
10.23919/ACC.2018.8431686

Linear Model Predictive Control for Schrödinger Equation*

Jukka-Pekka Humaloja**,1 and Stevan Dubljevic[2]

***Abstract*— The paper considers the finite-horizon constrained optimal control problem for Schrödinger equation with boundary controls and boundary observations. The plant is mapped from continuous to discrete time using the Cayley-Tustin transform, which preserves input-output–stability of the plant. The proposed transformation is structure and energy preserving and does not induce order reduction associated with the spatial discretization. The controller design setting leads to the finite horizon constrained quadratic regulator problem, which is easily realized and accounts in explicit manner for input and output/state constraints. The model predictive control (MPC) design is realized for Schrödinger equation and the results are illustrated with numerical simulations showing successful stabilization of Schrödinger equation with simultaneous satisfaction of input and output/state constraints.**

I. Introduction

A central concern in modern chemistry is controlled making and breaking of chemical molecular bonds. The state-of-the-art laser technology provides foundation for laser control in a favorable manner to alter the molecular dynamics phenomena. In particular, laboratory implementation and design are focused on successful laser field realizations capable of altering constructive and destructive interferences of the underlying molecular wave function [12].

In molecular control one seeks to achieve the best possible solution, and therefore it is natural to consider optimal control design methodologies as a starting point. Along this line, optimal control of quantum-mechanical systems was first considered by Dahleh, Peirce and Rabitz in [2], [9] where the finite-dimensional Schrödinger equation was considered under different circumstances. Later on, controller design problems for the finite-dimensional Schrödinger equation were considered in [7] by Mirrahimi and Rouchon and in [8] by Mirrahimi, Rouchon and Turinici. Recently, control of the infinite-dimensional Schrödinger equation has been considered, e.g., in [4], [10], [11]. The important notions of boundary applied actuation and observation in the context of Schrödinger equation have beed addressed in detailed manner in [14], due to the importance of accurate steering a system from initial to final observable state in the finite time.

* This work was carried out while the first author was visiting University of Alberta in 2017. The visit was funded by the doctoral program of the Faculty of Engineering and Natural Sciences of Tampere University of Technology.

** J-P. Humaloja is supported by the Academy of Finland Grant number 310489 held by Lassi Paunonen.

[1] J-P. Humaloja is with Tampere University of Technology, Mathematics, P.O. Box 553, 33101 Tampere, Finland jukka-pekka.humaloja@tut.fi

[2] S. Dubljevic is with University of Alberta, Chemicals & Materials Engineering Department, Edmonton, AB T6G 2V4, Canada stevan.dubljevic@ualberta.ca

In reality, the key to the laser control realization is accurate description of the Hamiltonian. In some cases for simple molecular species [2], [9] one can describe Hamiltonian with high accuracy and successfully apply design, while for polyatomic molecules and the subsequent design achieving acceptable accuracy is a very complex task. In addition, to this complexity, the control realizations with the presence of complex external fields contribute to the higher level of difficulty in realizing and implementing molecular control [13]. Besides these difficulties, one might need to account for the generation of undesirable chemical products (reflected in breaking the wrong chemical bonds). Along this line in [13], a theoretical method for optimization based control has been presented with application of multiple constraints and with guaranteed convergence to desired physical objectives. Motivated by this notion, we explore another design methodology that is optimal, explicitly accounts for constraints and is already well-known in control practice, a model predictive control [6], [17].

In particular, we consider a linear model predictive control design which has been successfully applied for similar types of distributive parameter systems [16]. It will be shown that one can extend the well-known design of the MPC to the setting of complex distributed parameter systems described by the Schrödinger equation and incorporate input and output/state constraints - as well as optimality - in the computationally fast and numerically realizable design setting. An additional benefit to our MPC design is that continuous Schrödinger equation model of the underlying plant is not subjected to any type of order reduction by spatial discretization and the issue of boundary applied actuation is realized by applying an appropriate exact boundary transformation [14]. Generalization to infinite-dimensional systems requires taking several theoretical aspects into account, even though here we omit some of the technical details.

The structure of this paper is as follows. In Section II, we present the general Cayley-Tustin time discretization scheme for distributed parameter systems which is symplectic and structure preserving [3]. In Section III, we present Schrödinger equation with boundary controls and boundary observations and apply the Cayley-Tustin discretization to the system. In Section IV, the model predictive control problem is presented and solved for the Schrödinger equation. Numerical simulations are presented as well. Finally, conclusions are presented in Section V.

Here $\mathcal{L}(X,Y)$ denotes the set of bounded linear operators from the normed space X to the normed space Y. The domain, kernel and resolvent of a linear operator A are denoted by $\mathcal{D}(A)$, $\mathcal{N}(A)$ and $\rho(A)$, respectively. For a linear operator $A : \mathcal{D}(A) \subset X \to X$ and a fixed $s_0 \in \rho(A)$, define the scale spaces $X_1 := (\mathcal{D}(A), \|(s_0 - A)\cdot\|)$ and $X_{-1} := \overline{(X, \|(s_0 - A)^{-1}\cdot\|)}$ [14, Sec. 2.10]. The scale spaces are related by $X_1 \subset X \subset X_{-1}$ where the inclusions are dense and with continuous embeddings. The extension of A to X_{-1} is denoted by A_{-1}.

II. Cayley-Tustin Time Discretization

Consider a linear infinite-dimensional system described by the following equations:

$$\dot{x}(\zeta, t) = Ax(\zeta, t) + Bu(t), \quad x(\zeta, 0) = x_0(\zeta) \tag{1a}$$

$$y(t) = Cx(\zeta, t) + Du(t). \tag{1b}$$

The state-space X, the input space U and the output space Y are assumed to be Hilbert spaces. The linear operator $A : \mathcal{D}(A) \subset X \to X$ is the generator of a C_0-semigroup and for the other operators we assume that $B \in \mathcal{L}(U, X_{-1})$, $C \in \mathcal{L}(X_1, Y)$ and $D \in \mathcal{L}(U, Y)$.

Given a discretization parameter $h > 0$, a Crank-Nicolson type time discretization of (1) is given by

$$\frac{x(\cdot, ih) - x(\cdot, (i-1)h)}{h} \approx A\frac{x(\cdot, ih) + x(\cdot, (i-1)h)}{2} + Bu(ih)$$

$$y(ih) \approx C\frac{x(\cdot, ih) + x(\cdot, (i-1)h)}{2} + Du(ih)$$

for $i \geq 1$. Approximating $u(ih)$ by $u_i^h/\sqrt{h}$ (using a chosen sampling), it has been shown in [5] that the Cayley-Tustin discretization is a convergent time discretization scheme for a general class of input-output stable systems satisfying $\dim U = \dim Y = 1$ such that $y_i^h/\sqrt{h}$ converges to $y(ih)$ in several different ways. A straightforward manipulation yields the Cayley-Tustin transform $(A, B, C, D) \to (A_d, B_d, C_d, D_d)$ by

$$S = \begin{bmatrix} A_d & B_d \\ C_d & D_d \end{bmatrix} := \begin{bmatrix} (\delta + A)(\delta - A)^{-1} & \sqrt{2\delta}(\delta - A_{-1})^{-1}B \\ \sqrt{2\delta}C(A - \delta)^{-1} & G(\delta) \end{bmatrix}$$

where $G(\delta) := C(\delta - A_{-1})^{-1}B + D$ denotes the transfer function of the system and $\delta = 2/h$ which needs to be in $\rho(A)$. It is easy to see that the operator A_d can be equivalently expressed as $A_d = -I + 2\delta(\delta - A)^{-1}$.

III. Schrödinger Equation

In this section, we apply the Cayley-Tustin time discretization to the boundary controlled Schrödinger equation on the unit interval $\zeta \in [0, 1]$. The system is given for $x(\zeta, 0) = x_0(\zeta)$ by

$$\frac{\partial}{\partial t}x(\zeta, t) = j\frac{\hbar}{2m}\frac{\partial^2}{\partial\zeta^2}x(\zeta, t) - vx(\zeta, t) \tag{2a}$$

$$\frac{\partial}{\partial\zeta}x(0, t) = 0 \tag{2b}$$

$$\frac{\partial}{\partial\zeta}x(1, t) = u(t) \tag{2c}$$

$$x(0, t) = y(t) \tag{2d}$$

where $\hbar$ is the reduced Planck constant, m is the mass of the particle, $v > 0$ accounts for the potential energy of the particle and $u \in U, y \in Y$ are boundary control and boundary observation signals, respectively, where $U = Y := \mathbb{C}$.

In order to write the system (2) in the usual state-space form (1), we define an operator $\mathcal{A}$ by

$$\mathcal{A}x := j\frac{\hbar}{2m}\frac{\partial^2}{\partial\zeta^2}x - vx$$

with domain

$$\mathcal{D}(\mathcal{A}) = \left\{x \in L_2(0, 1; \mathbb{C}) : \tfrac{\hbar}{2m}x \in H^2(0, 1; \mathbb{C}),\ \tfrac{\partial x}{\partial\zeta}(0) = 0\right\}.$$

Furthermore, we define a boundary control operator $\mathcal{B}$ by

$$\mathcal{B}x(\cdot, t) := \frac{\partial}{\partial\zeta}x(1, t)$$

with domain $\mathcal{D}(\mathcal{B}) := \mathcal{D}(\mathcal{A})$. The operator $\mathcal{A}$ corresponds to the port-Hamiltonian formulation of Schrödinger equation (see, e.g., [1, Ex. 2.18]), and [1, Thm. 2.3] implies that the operator $A := \mathcal{A}|_{\mathcal{N}(\mathcal{B})}$ with domain $\mathcal{D}(A) = \mathcal{D}(\mathcal{A}) \cap \mathcal{N}(\mathcal{B})$, i.e., the restriction of $\mathcal{A}$ to the kernel of $\mathcal{B}$, generates a C_0-semigroup.

The aforementioned implies that the pair $(\mathcal{A}, \mathcal{B})$ is a boundary control system in the sense of [14, Def. 10.1.1]. Thus, by [14, Prop. 10.1.2, Rem. 10.1.4] there exists a unique operator $B \in \mathcal{L}(U, X_{-1})$ such that the system (2) can be equivalently written as

$$\dot{x}(\zeta, t) = Ax(\zeta, t) + Bu(t), \quad x(0) = x_0 \tag{3a}$$

$$y(t) = \mathcal{C}x(\zeta, t) \tag{3b}$$

where $\mathcal{C} \in \mathcal{L}(X_1, Y)$ with domain $\mathcal{D}(\mathcal{C}) := \mathcal{D}(\mathcal{A})$ is defined as $\mathcal{C}x(\cdot, t) := x(0, t)$ so that (3b) corresponds to (2d).

The aforementioned operator B can be found by solving the abstract elliptic problem [14, Rem. 10.1.5] $\mathcal{A}f = sf$, $\mathcal{B}f = u$ for any $s \in \rho(A)$ and $u \in U$. The solution is unique and satisfies $f = (s - A_{-1})^{-1}Bu$. A direct computation shows that for any $s \in \rho(A)$ and $u \in U$, the solution is given by

$$f_s(\zeta) = \frac{1}{c_s}\frac{\cosh(c_s\zeta)}{\sinh(c_s)}u \tag{4}$$

where $c_s = \frac{1-j}{\sqrt{2}}\sqrt{\frac{2m}{\hbar}(s + v)}$, and thus, the operator B is obtained by $Bu = (s - A_{-1})f_s(\zeta)$.

A. Discretized Operators

In this section, we will compute the discrete time linear system operators (A_d, B_d, C_d, D_d). In order to do that, let us find the resolvent of the operator A by considering the homogeneous PDE

$$\dot{x}(\zeta, t) = Ax(\zeta, t), \quad x(\zeta, 0) = x_0(\zeta) \tag{5}$$

where A is the same as in (3). Applying Laplace transform to (5) yields

$$sx(\zeta, s) - x(\zeta, 0) = j\frac{\hbar}{2m}\frac{\partial^2}{\partial\zeta^2}x(\zeta, t) - vx(\zeta, t), \tag{6}$$

that is,

$$\frac{\partial^2}{\partial\zeta^2}x(\zeta, t) = -j\frac{2m}{\hbar}sx(\zeta, s) - jv\frac{2m}{\hbar}x(\zeta, s) + j\frac{2m}{\hbar}x(\zeta, 0),$$

which can be equivalently written as

$$\frac{\partial}{\partial\zeta}\begin{bmatrix}x(\zeta,t)\\ \partial_\zeta x(\zeta,t)\end{bmatrix}=\begin{bmatrix}0 & 1\\ -j\frac{2m}{\hbar}(s+v) & 0\end{bmatrix}\begin{bmatrix}x(\zeta,t)\\ \partial_\zeta x(\zeta,t)\end{bmatrix}+\begin{bmatrix}0\\ j\frac{2m}{\hbar}x(\zeta,0)\end{bmatrix}.$$

The above system is an ODE of the form

$$\partial_\zeta\overline{X}(\zeta,s)=\overline{A}\overline{X}(\zeta,s)+\overline{B}(\zeta),$$

the solution of which is given by

$$\overline{X}(\zeta,s)=e^{\overline{A}\zeta}\overline{X}(0,s)+\int_0^\zeta e^{\overline{A}(\zeta-\eta)}\overline{B}(\eta)d\eta. \tag{7}$$

A direct computation shows that

$$e^{\overline{A}\zeta}=\begin{bmatrix}\cosh(c_s\zeta) & \frac{1}{c_s}\sinh(c_s\zeta)\\ c_s\sinh(c_s\zeta) & \cosh(c_s\zeta)\end{bmatrix}$$

where again $c_s=\frac{1-j}{\sqrt{2}}\sqrt{\frac{2m}{\hbar}(s+v)}$.

By the definition of $\mathcal{D}(A)$, we must have $\partial_\zeta x(0,s)=\partial_\zeta x(1,s)=0$, which yields that in (7), $\overline{X}(0,s)$ is given by

$$\overline{X}(0,s)=\begin{bmatrix}-\frac{1}{c_s\sinh(c_s)}\int_0^1 j\frac{2m}{\hbar}\cosh(c_s(1-\eta))x(\eta,0)d\eta\\ 0\end{bmatrix}.$$

Finally, the solution of (6) is given by

$$\begin{aligned}x(\zeta,s)&=-\frac{j}{c_s}\frac{2m}{\hbar}\frac{\cosh(c_s\zeta)}{\sinh(c_s)}\int_0^1\cosh(c_s(1-\eta))x(\eta,0)d\eta\\&\quad+\frac{j}{c_s}\frac{2m}{\hbar}\int_0^\zeta\sinh(c_s(\zeta-\eta))x(\eta,0)d\eta\\&:=(s-A)^{-1}x(\zeta,0)\end{aligned} \tag{8}$$

which yields the expression for the resolvent operator.

Now that we have derived an expression for the resolvent of A, a direct computation shows that

$$\begin{aligned}A_dx(\zeta)&=-x(\zeta)+\frac{2\delta j}{c_\delta}\frac{2m}{\hbar}\int_0^\zeta\sinh(c_\delta(\zeta-\eta))x(\eta)d\eta\\&\quad-\frac{2\delta j}{c_\delta}\frac{2m}{\hbar}\frac{\cosh(c_\delta\zeta)}{\sinh(c_\delta)}\int_0^1\cosh(c_\delta(1-\eta))x(\eta)d\eta.\end{aligned} \tag{9}$$

In order to compute B_d, we choose $s=\delta$ in (4) so that $Bu=(\delta-A_{-1})f_\delta(\zeta)$, and we obtain $(\delta-A_{-1})^{-1}Bu=f_\delta(\zeta)$, and thus,

$$B_d=\frac{\sqrt{2\delta}}{c_\delta}\frac{\cosh(c_\delta\zeta)}{\sinh(c_\delta)}. \tag{10}$$

The operator C_d is simply given by

$$C_dx(\zeta)=-\frac{\sqrt{2\delta}j}{c_\delta}\frac{2m}{\hbar}\frac{1}{\sinh(c_\delta)}\int_0^1\cosh(c_\delta(1-\eta))x(\eta)d\eta \tag{11}$$

and finally, the operator $D_d=G(\delta)=C(\delta-A_{-1})^{-1}B$ is given by

$$D_d=\frac{1}{c_\delta}\frac{1}{\sinh(c_\delta)}. \tag{12}$$

We note that

$$\lim_{s\to\infty}G(s)=0,$$

which implies that the system (3) is in fact a *regular linear system* (see, e.g., [15]) and, in particular, well-posed.

B. Adjoint Operators

In this section, we will compute the adjoints of the operators (A_d,B_d,C_d,D_d). We note that the state space $X:=L^2(0,1;\mathbb{C})$ is equipped with the inner product

$$\langle f,g\rangle_X=\int_0^1 f^*(\zeta)g(\zeta)d\zeta,$$

and the input and output spaces $U=Y:=\mathbb{C}$ are equipped with the usual complex inner product $\langle u_1,u_2\rangle_{\mathbb{C}}=u_1^*u_2$.

By definition, the adjoint P^* of an operator P satisfies $\langle Px,y\rangle=\langle x,P^*y\rangle$ with respect to the corresponding inner products. Now for A_d, we obtain

$$\begin{aligned}\langle A_dx,z\rangle_X&=-\int_0^1x^*(\zeta)z(\zeta)d\zeta\\&\quad+\int_0^1\int_0^1\frac{4m\delta j}{c_\delta^*\hbar}\frac{\cosh(c_\delta^*\zeta)}{\sinh(c_\delta^*)}\cosh(c_\delta^*(1-\eta))x^*(\eta)z(\zeta)d\eta d\zeta\\&\quad-\int_0^1\int_0^\zeta\frac{4m\delta j}{c_\delta^*\hbar}\sinh(c_\delta^*(\zeta-\eta))x^*(\eta)z(\zeta)d\eta d\zeta\\&=-\int_0^1x^*(\zeta)z(\zeta)d\zeta\\&\quad+\int_0^1x^*(\zeta)\int_0^1\frac{4m\delta j}{c_\delta^*\hbar}\frac{\cosh(c_\delta^*\eta)}{\sinh(c_\delta^*)}\cosh(c_\delta^*(1-\zeta))z(\eta)d\eta d\zeta\\&\quad-\int_0^1x^*(\zeta)\int_\zeta^1\frac{4m\delta j}{c_\delta^*\hbar}\sinh(c_\delta^*(\eta-\zeta))z(\eta)d\eta d\zeta\\&=\langle x,A_d^*z\rangle_X,\end{aligned}$$

so we have

$$\begin{aligned}A_d^*x(\zeta)&=-x(\zeta)-\frac{2\delta j}{c_\delta^*}\frac{2m}{\hbar}\int_\zeta^1\sinh(c_\delta^*(\eta-\zeta))x(\eta)d\eta\\&\quad+\frac{2\delta j}{c_\delta^*}\frac{2m}{\hbar}\frac{\cosh(c_\delta^*(1-\zeta))}{\sinh(c_\delta^*)}\int_0^1\cosh(c_\delta^*\eta)x(\eta)d\eta.\end{aligned} \tag{13}$$

For B_d we obtain

$$\langle B_du,x\rangle_X=\langle u,\langle B_d,x\rangle_X\rangle_{\mathbb{C}}=\langle u,B_d^*x\rangle_{\mathbb{C}},$$

that is,

$$B_d^*x=\langle B_d,x\rangle_X=\frac{\sqrt{2\delta}}{c_\delta^*}\int_0^1\frac{\cosh(c_\delta^*\zeta)}{\sinh(c_\delta^*)}x(\zeta)d\zeta. \tag{14}$$

Similarly for C_d we have

$$\begin{aligned}\langle C_dx,y\rangle_{\mathbb{C}}&=\int_0^1y\frac{\sqrt{2\delta}j}{c_\delta^*}\frac{2m}{\hbar}\frac{\cosh(c_\delta^*(1-\eta))}{\sinh(c_\delta^*)}x^*(\eta)d\eta\\&=\langle x,C_d^*y\rangle_X,\end{aligned}$$

where

$$C_d^*=\frac{\sqrt{2\delta}j}{c_\delta^*}\frac{2m}{\hbar}\frac{\cosh(c_\delta^*(1-\zeta))}{\sinh(c_\delta^*)}. \tag{15}$$

Finally, the adjoint D_d^* of D_d is simply given by

$$D_d^*=\frac{1}{c_\delta^*}\frac{1}{\sinh(c_\delta^*)}. \tag{16}$$

IV. The Model Predictive Control Problem

In the case of complex scalar input and output spaces, the objective function with constraints at a given sampling time k is given by

$$\begin{aligned}\min_u \sum_{i=0}^{\infty} & y^*(k+i)Qy(k+i)+u^*(k+i+1)Ru(k+i+1)\\ s.t.\quad & x(\zeta,k+i)=A_d x(\zeta,k+i-1)+B_d u(k+i)\\ & y(k+i)=C_d x(\zeta,k+i)+D_d u(k+i)\\ & \operatorname{Re}u_{\min}\leq \operatorname{Re}u(k+i)\leq \operatorname{Re}u_{\max}\\ & \operatorname{Im}u_{\min}\leq \operatorname{Im}u(k+i)\leq \operatorname{Im}u_{\max}\\ & \operatorname{Re}y_{\min}\leq \operatorname{Re}y(k+i)\leq \operatorname{Re}y_{\max}\\ & \operatorname{Im}y_{\min}\leq \operatorname{Im}y(k+i)\leq \operatorname{Im}y_{\max}\end{aligned}$$

where Q and R are positive constants. Note that as the input and output spaces are complex, we need to consider lower and upper bounds separately for the real and imaginary parts of u and y. However, in the following we will restrict to considering only real inputs as complex inputs are not implementable in practice. Thus, in the following we treat the input space U as $\mathbb{R}$.

The aforementioned infinite-horizon open-loop objective function can be cast as a finite-horizon open-loop objective function under the assumption that the input u is zero beyond the control horizon N, i.e., $u(k+N)=0$. Additionally, an output penalty term needs to be included. Under the assumption of observability, the output terminal penalty can be expressed as a terminal state penalty term $\langle x(k+N-1),\bar{Q}x(k+N-1)\rangle$, and the finite horizon open-loop objective function can the be written as

$$\min_{U_k} Y_k^*QY_k+U_k^TRU_k+\langle x(\zeta,k+N-1),\bar{Q}x(\zeta,k+N-1)\rangle_X \tag{17}$$

where $U_k\in\mathbb{R}^{N-1}, Y_k\in\mathbb{C}^{N-1}$ are given by

$$\begin{aligned}U_k&=\begin{bmatrix}u(k+1) & u(k+2) & \dots & u(k+N-1)\end{bmatrix}\\ Y_k&=\begin{bmatrix}y(k) & y(k+1) & \dots & y(k+N-2)\end{bmatrix}.\end{aligned}$$

In the preceding, the operator $\bar{Q}$ can be calculated from a self-adjoint solution of the following discrete Lyapunov equation (see [16])

$$A_d^*\bar{Q}A_d-\bar{Q}=-C_d^*QC_d. \tag{18}$$

We will address solving (18) in more detail in Section IV-A.

A straightforward manipulation of the objective function given in (17) yields the following finite-dimensional quadratic optimization problem

$$\begin{aligned}\min_{U_k}\quad & U_k^THU_k+2\operatorname{Re}\left(U_k^TPx(\zeta,k)\right)\\ & +\langle x(\zeta,k),\bar{Q}x(\zeta,k)\rangle_X+\langle y(k),Qy(k)\rangle_{\mathbb{C}}\end{aligned} \tag{19}$$

where $H\in\mathbb{C}^{N-1\times N-1}$ is self-adjoint given by

$$h_{m,n}=\begin{cases}D_d^*QD_d+B_d^*\bar{Q}B_d+R & \text{for } m=n\\ D_d^*QC_dA_d^{m-n-1}B_d+B_d^*\bar{Q}A_d^{m-n}B_d & \text{for } m>n\\ h_{n,m}^* & \text{for } m<n\end{cases}$$

and $P\in\mathcal{L}(X,\mathbb{C}^{N-1})$ is given by

$$P=\begin{bmatrix}D_d^*QC_d+B_d^*\bar{Q}A_d\\ D_d^*QC_dA_d+B_d^*\bar{Q}A_d^2\\ \vdots\\ D_d^*QC_dA_d^{N-2}+B_d^*\bar{Q}A_d^{N-1}\end{bmatrix}.$$

Note that since we are restricted to real inputs, we only need to consider the real parts of H and $Px(\zeta,k)$. The objective function given in (19) is subjected to constraints

$$\begin{aligned}U_{\min}&\leq U_k\leq U_{\max}\\ \operatorname{Re}Y_{\min}&\leq \operatorname{Re}\left(SU+Tx(\zeta,k)\right)\leq \operatorname{Re}Y_{\max}\\ \operatorname{Im}Y_{\min}&\leq \operatorname{Im}\left(SU+Tx(\zeta,k)\right)\leq \operatorname{Im}Y_{\max},\end{aligned}$$

which can be written in the form

$$\begin{bmatrix}I\\ -I\\ \operatorname{Re}S\\ \operatorname{Im}S\\ -\operatorname{Re}S\\ -\operatorname{Im}S\end{bmatrix}U_k\leq\begin{bmatrix}U_{\max}\\ -U_{\min}\\ \operatorname{Re}\left(Y_{\max}-Tx(\zeta,k)\right)\\ \operatorname{Im}\left(Y_{\max}-Tx(\zeta,k)\right)\\ -\operatorname{Re}\left(Y_{\max}-Tx(\zeta,k)\right)\\ -\operatorname{Im}\left(Y_{\max}-Tx(\zeta,k)\right)\end{bmatrix}$$

where $S\in\mathbb{C}^{N-1\times N-1}$ is lower triangular given by

$$s_{m,n}=\begin{cases}D_d & \text{for } m=n\\ C_dA_d^{m-n-1}B_d & \text{for } m>n\\ 0 & \text{for } m<n\end{cases}$$

and $T\in\mathcal{L}(X,\mathbb{C}^{N-1})$ is given by

$$T=\begin{bmatrix}C_d\\ C_dA_d\\ \vdots\\ C_dA_d^{N-2}\end{bmatrix}.$$

A. A Solution of the Lyapunov Equation

Before going into simulations regarding model predictive control of Schrödinger equation, we will derive a self-adjoint solution for the discrete time Lyapunov equation (18). It has been shown in [16] that the solutions of the discrete time Lyapunov equation coincide with the solutions of the continuous time Lyapunov equation

$$A^*\bar{Q}+\bar{Q}A=-\mathcal{C}^*Q\mathcal{C}.$$

We will find a solution of the continuous time Lyapunov equation by utilizing the spectral presentation of A.

Consider the eigenvalue equation

$$A\phi_k=\lambda_k\phi_k$$

for Schrödinger equation considered in Section III. A direct computation shows that the eigenvectors ϕ_k are of the form

$$\phi_k=\alpha\cosh\left(\frac{1-j}{\sqrt{2}}\sqrt{\frac{2m}{\hbar}(v+\lambda_k)}\zeta\right)$$

which satisfy $\partial_\zeta\phi_k(0)=0$. Since $\phi_k\in\mathcal{D}(A)$, ϕ_k must also satisfy $\partial_\zeta\phi_k(1)=0$, which yields

$$0=\alpha\frac{1-j}{\sqrt{2}}\sqrt{\frac{2m}{\hbar}(v+\lambda_k)}\sinh\left(\frac{1-j}{\sqrt{2}}\sqrt{\frac{2m}{\hbar}(v+\lambda_k)}\right).$$

Since $\sinh(z) = 0$ holds for $z = jk\pi$, $n \in \mathbb{Z}$, we obtain that the eigenvalues of A are given by

$$\lambda_k = -j\frac{\hbar}{2m}(k\pi)^2 - v$$

for $k \in \mathbb{N}_0$, which implies that A is the generator of an exponentially stable C_0-semigroup. The eigenvectors ϕ_k are now given by

$$\phi_k = \alpha\cosh(jk\pi) = \alpha\cos(k\pi)$$

which form an orthonormal basis of X with the choices $\alpha = 1$ for $k = 0$ and $\alpha = \sqrt{2}$ otherwise.

Let us now apply the continuous Lyapunov equation to an arbitrary $x \in \mathcal{D}(A)$:

$$A^*\bar{Q}x + \bar{Q}Ax = -\mathcal{C}^*Q\mathcal{C}x.$$

Representing x in the basis formed by the eigenvectors of A yields

$$\sum_{k=0}^{\infty}\left(A^*\bar{Q}\langle x,\phi_k\rangle\phi_k + \bar{Q}A\langle x,\phi_k\rangle\phi_k + \mathcal{C}^*Q\mathcal{C}\langle x,\phi_k\rangle\phi_k\right) = 0,$$

that is,

$$\sum_{k=0}^{\infty}\left((A^* + \lambda_k)\bar{Q}\langle x,\phi_k\rangle\phi_k + \mathcal{C}^*Q\mathcal{C}\langle x,\phi_k\rangle\phi_k\right) = 0,$$

which especially holds if

$$\bar{Q}\langle x,\phi_k\rangle\phi_k = (-\lambda_k - A^*)^{-1}\mathcal{C}^*Q\mathcal{C}\langle x,\phi_k\rangle\phi_k \tag{20}$$

for all $k \in \mathbb{N}_0$. We note that as A is densely defined and $-\lambda_k^* \in \rho(A)$, we have by [14, Prop. 2.8.4] that $(-\lambda_k - A^*)^{-1} = \left((-\lambda_k^* - A)^{-1}\right)^*$. Now summation over k in (20) yields a solution:

$$\bar{Q}x = \sum_{k=0}^{\infty}\langle x,\phi_k\rangle\left(\mathcal{C}(-\lambda_k^* - A)^{-1}\right)^* Q\mathcal{C}\phi_k \tag{21}$$

where we have based on C_d^* that

$$\left(\mathcal{C}(s - A)^{-1}\right)^* = \frac{2mj}{c_s^*\hbar}\frac{\cosh(c_s^*(1-\zeta))}{\sinh(c_s^*)}$$

for all $s \in \rho(A)$.

We note that as $\mathcal{C}\phi_k = \alpha$ and $\mathcal{C}(-\lambda_k^* - A)^{-1}$ is uniformly bounded for all $k \in \mathbb{N}_0$, (21) is a convergent series. Thus, denoting the Mth partial sum of (21) by $\bar{Q}_M$, we obtain for every $x \in \mathcal{D}(A)$ that $\lim_{M\to\infty} \|(\bar{Q} - \bar{Q}_M)x\| \to 0$, which implies that the solution $\bar{Q}x$ can be evaluated to arbitrary precision $\epsilon > 0$ by choosing a sufficiently large (finite) M. A sufficiently large value for M can be determined, e.g., by numerical experiments, as done in the simulation of the following section.

B. Simulation Results for Schrödinger Equation

In this section, we present simulation results for Schrödinger equation considered in Section III under the model predictive control law (19). For the simulation, we consider Schrödinger equation for a free electron, so in atomic units the parameters in (2) are given by $m = 1$, $\hbar = 1$ and we choose $v = 1$.

The input and output weights are chosen as $R = 10$ and $Q = 5$, respectively. For the Cayley-Tustin time discretization, we choose $h = 0.05$, so $\delta = 40$. Furthermore, $d\zeta = 2^{-9}$ is chosen for numerical integration. The initial condition is $x_0(\zeta) = \cos(\pi\zeta)$ and the model predictive control horizon is $N = 10$. For computation of the function $\bar{Q}$, the series in (21) is approximated by summing the first $M = 101$ terms. The input and output constraints are given as $u_{\min} = -0.3$, $u_{\max} = 0.03$, $y_{\min} = -0.1 - 0.2j$ and $y_{\max} = 0.2 + 0.05j$.

The input profile of the simulation and the input constraints are shown in Figure 1. Figure 2 shows the comparison between the output profiles of the open- and closed-loop systems under model predictive control, along with output constraints. One can see from these figures that a maximal control effort is required near the beginning to keep the real and imaginary parts of the output signal within the allowed limits. Thereafter virtually no control is imposed nor required.

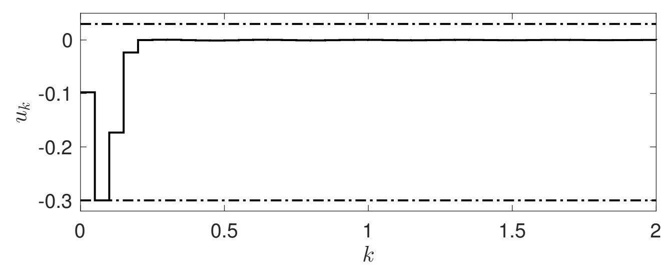

Fig. 1. Input profile model predictive control law under input and output constraints (solid line) and input constraints (dash-dot-line).

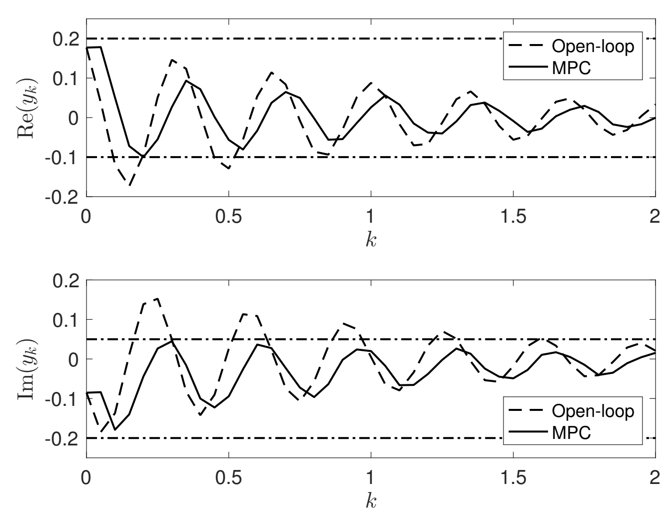

Fig. 2. Comparison between the profile of the closed-loop system under model predictive control (solid line) and the profile of the open-loop system (dashed line). Output constraints are shown in dash-dot-line

In Figures 3 and 4 the state profiles of the open- and closed-loop systems, respectively, are presented for comparison. The effect of control can be seen here as well, as the state under the model predictive control law in Figure 4 decays in the beginning faster than the state of the open-loop system. Even thought both the MPC and the open-loop states decay asymptotically to zero due to the system being exponentially stable, the most substantial difference between the open-loop and the MPC behaviors – as seen in Figure 2 – is that MPC keeps the output within the given constraints while the open-loop output violates them.

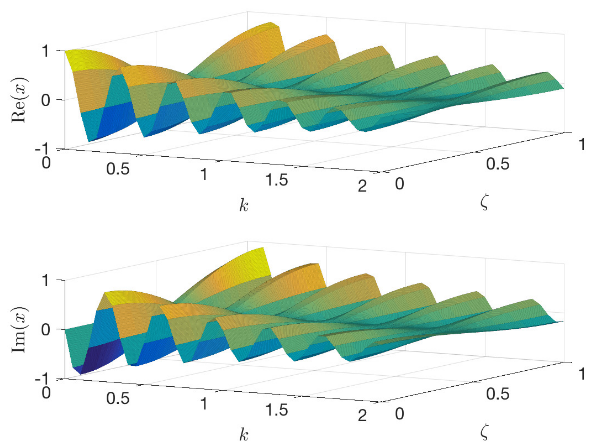

Fig. 3. The evolution of the state profile of the open-loop system.

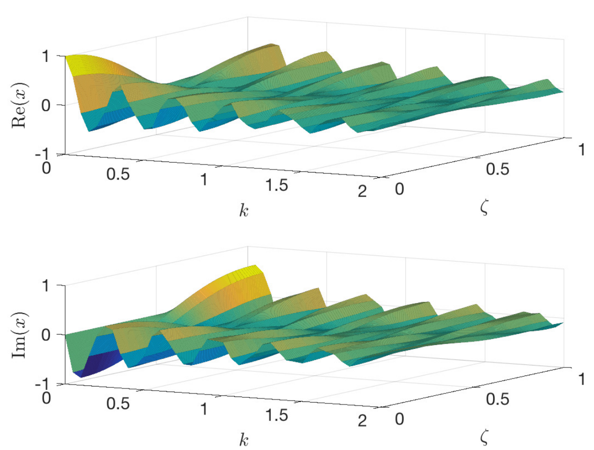

Fig. 4. The evolution of the state profile under the model predictive control law with input and output constraints.

V. Conclusions

We considered the finite-horizon constrained optimal control problem for the Schrödinger equation with boundary controls and boundary observations. The plant was mapped from continuous to discrete time using the Cayley-Tustin transformation, which is a convergent time discretization scheme for a rather general class of systems. No spatial approximations were required in the process. The control problem was solved for Schrödinger equation and the results were illustrated with numerical simulations.

References

[1] B. Augner and B. Jacob. Stability and stabilization of infinite-dimensional linear port-Hamiltonian systems. *Evolution Equations and Control Theory*, 3(2):207–229, 2014.

[2] M. A. Dahleh, A. P. Peirce, and H. Rabitz. Optimal control of uncertain quantum systems. *Phys. Rev. A*, 42(3):1065–1079, 1990.

[3] E. Hairer, C. Lubich, and G. Wanner. *Geometric Numerical Integration: Structure-Preserving Algorithms for Ordinary Differential Equations*, volume 31 of *Springer Series in Computational Mathematics*. Springer, Berlin, 2002.

[4] S. W. Hansen. Exact boundary controllability of a Schrödinger equation with an internal point mass. In *American Control Conference (ACC)*, pages 3809–3814, 2017.

[5] V. Havu and J. Malinen. The Cayley transform as a time discretization scheme. *NFAO*, 28(7-8):825–851, 2007.

[6] D. Q. Mayne. Model predictive control: Recent developments and future promise. *Automatica*, 50(12):2967 – 2986, 2014.

[7] M. Mirrahimi and P. Rouchon. Controllability of quantum harmonic oscillators. *IEEE Trans. Automat. Control*, 49(5):745–747, 2004.

[8] M. Mirrahimi, P. Rouchon, and G. Turinici. Lyapunov control of bilinear Schrödinger equations. *Automatica*, 41(11):1987 – 1994, 2005.

[9] A. P. Peirce, M. A. Dahleh, and H. Rabitz. Optimal control of quantum-mechanical systems: Existence, numerical approximation, and applications. *Phys. Rev. A*, 37(12):4950–4964, 1988.

[10] Y. Privat, E. Trélat, and E. Zuazua. Optimal shape and location of sensors or actuators in PDE models. In *American Control Conference (ACC)*, pages 4063–4068, 2014.

[11] Y. Privat, E. Trélat, and E. Zuazua. Optimal observability of the multi-dimensional wave and Schrödinger equations in quantum ergodic domains. *JEMS*, 18(5):1043–1111, 2016.

[12] H. Rabitz and W. Zhu. Optimal control of molecular motion: Design, implementation, and inversion. *Accounts of Chemical Research*, 33(8):572–578, 2000. PMID: 10955988.

[13] C.-C. Shu, T.-S. Ho, X. Xing, and H. Rabitz. Frequency domain quantum optimal control under multiple constraints. *Phys. Rev. A*, 93:033417, Mar 2016.

[14] M. Tucsnak and G. Weiss. *Observation and Control for Operator Semigroups*. Birkhäuser Verlag AG, 2009.

[15] G. Weiss. Transfer functions of regular linear systems. Part I: Characterzations of regularity. *Trans. Amer. Math. Soc.*, 342(2):827–854, 1994.

[16] Q. Xu and S. Dubljevic. Linear model predictive control for transport-reaction processes. *AIChE J.*, 63:2644–2659, 2017.

[17] M. N. Zeilinger, D. M. Raimondo, A. Domahidi, M. Morari, and C. N. Jones. On real-time robust model predictive control. *Automatica*, 50(3):683 – 694, 2014.